

Semi-Supervised Learning via Cross-Prediction-Powered Inference for Wireless Systems

Houssem Sifaou and Osvaldo Simeone

Abstract

In many wireless application scenarios, acquiring labeled data can be prohibitively costly, requiring complex optimization processes or measurement campaigns. Semi-supervised learning leverages unlabeled samples to augment the available dataset by assigning synthetic labels obtained via machine learning (ML)-based predictions. However, treating the synthetic labels as true labels may yield worse-performing models as compared to models trained using only labeled data. Inspired by the recently developed prediction-powered inference (PPI) framework, this work investigates how to leverage the synthetic labels produced by an ML model, while accounting for the inherent bias with respect to true labels. To this end, we first review PPI and its recent extensions, namely tuned PPI and cross-prediction-powered inference (CPPI). Then, we introduce a novel variant of PPI, referred to as tuned CPPI, that provides CPPI with an additional degree of freedom in adapting to the quality of the ML-based labels. Finally, we showcase two applications of PPI-based techniques in wireless systems, namely beam alignment based on channel knowledge maps in millimeter-wave systems and received signal strength information-based indoor localization. Simulation results show the advantages of PPI-based techniques over conventional approaches that rely solely on labeled data or that apply standard pseudo-labeling strategies from semi-supervised learning. Furthermore, the proposed tuned CPPI method is observed to guarantee the best performance among all benchmark schemes, especially in the regime of limited labeled data.

The authors are with the King's Communications, Learning & Information Processing (KCLIP) lab within the Centre for Intelligent Information Processing Systems (CIIPS), Department of Engineering, King's College London, WC2R 2LS London, U.K. (e-mail: houssem.sifaou@kcl.ac.uk; osvaldo.simeone@kcl.ac.uk).

The work of H. Sifaou and O. Simeone was partially supported by the European Union's Horizon Europe project CENTRIC (101096379). O. Simeone was also supported by the Open Fellowships of the EPSRC (EP/W024101/1) by the EPSRC project (EP/X011852/1), and by Project REASON, a UK Government funded project under the Future Open Networks Research Challenge (FONRC) sponsored by the Department of Science Innovation and Technology (DSIT).

Index Terms

Prediction-powered inference, semi-supervised learning, channel knowledge map, indoor localization

I. INTRODUCTION

A. Context and Motivation

Next-generation wireless systems are expected to rely extensively on machine learning (ML) and data-driven decision-making [1]–[3]. Optimizing effective ML algorithms hinges on the availability of high-quality labeled data. However, obtaining labeled data is a challenging task in numerous wireless scenarios due to the need to run time-consuming optimizations [4], [5] or to collect data via on-air transmission [6], [7]. Semi-supervised learning via pseudo-labeling provides a promising alternative by leveraging synthetic labels produced by ML models for unlabeled data [8]–[17]. However, predictions generated by ML models may be of insufficient quality. Therefore, making reliable use of synthetic labels requires an additional effort to reduce the bias caused by the discrepancy between synthetic and real labels. This is the focus of this work.

Specifically, we consider a semi-supervised setting in which unlabeled data \tilde{X} are abundant, while labels Y are difficult to obtain. The goal is to learn a parameter vector θ . As illustrated in Fig. 1, we assume the availability of an ML model $f(X)$ that can assign a synthetic label $f(\tilde{X})$ to any input \tilde{X} . Assuming the model $f(X)$ to be pretrained, conventional semi-supervised learning schemes would augment the dataset with the synthetic data $(\tilde{X}, f(\tilde{X}))$ obtained from the unlabeled data \tilde{X} to estimate parameter θ [19].

Note that we do not explore here semi-supervised methods that aim at extracting information from the covariate distribution, e.g., via generative models or via unsupervised pre-training; or that augment the data sets by generating new samples (\tilde{X}, Y) based on manipulation of existing inputs X (see, e.g., [20]). Such methods are complementary to the pseudo-labeling formulation adopted here and may be potentially combined with pseudo-labeling [18].

The *prediction-powered inference* (PPI) framework, introduced in [18], takes a different approach, using the limited labeled data to estimate the bias $\Delta^{\text{PP}}(\theta)$ caused by the mismatch

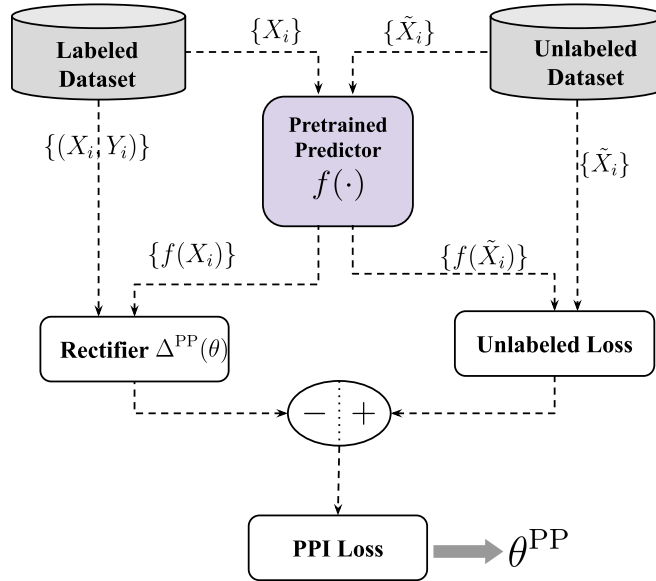


Fig. 1. Illustration of the original PPI scheme [18]: Using the labeled data and a pre-trained model $f(\cdot)$, the rectifier term $\Delta^{\text{PP}}(\theta) = \frac{1}{n} \sum_{i=1}^n [\ell_\theta(X_i, f(X_i)) - \ell_\theta(X_i, Y_i)]$ is evaluated to estimate the prediction bias of the model $f(\cdot)$. This term is subtracted from the unlabeled loss $\frac{1}{N} \sum_{i=1}^N \ell_\theta(\tilde{X}_i, f(\tilde{X}_i))$, obtaining the PPI loss $L^{\text{PP}}(\theta)$ in (1).

between true labels Y and predicted labels $f(\tilde{X})$. Using this *rectifier* term $\Delta^{\text{PP}}(\theta)$, given an unlabeled dataset $\{\tilde{X}_i\}_{i=1}^N$, PPI estimates the population loss as

$$L^{\text{PP}}(\theta) = \frac{1}{N} \sum_{i=1}^N \ell_\theta(\tilde{X}_i, f(\tilde{X}_i)) - \Delta^{\text{PP}}(\theta), \quad (1)$$

where $\ell_\theta(X, Y)$ is a loss function dependent on the parameter θ under optimization. The PPI approach is illustrated in Fig. 1.

The original PPI method may not necessarily improve over a baseline empirical risk minimization (ERM) that disregards unlabeled data. To obviate this issue, reference [21] introduced *tuned PPI*, which adapts the use of unlabeled data depending on the quality of the predictions.

Both PPI in [18] and tuned PPI in [21] assume the availability of a pretrained ML model $f(X)$ for annotating the unlabeled data. To alleviate this assumption, the authors in [22] proposed *cross-prediction-powered inference* (CPPI). In CPPI, the labeled data must be shared between the tasks of training the model $f(X)$ and evaluating a rectifier $\Delta(\theta)$. Note that, unlike semi-supervised methods such as co-training techniques, this approach does not require the extraction of different “views” from the input, as done in image processing [23].

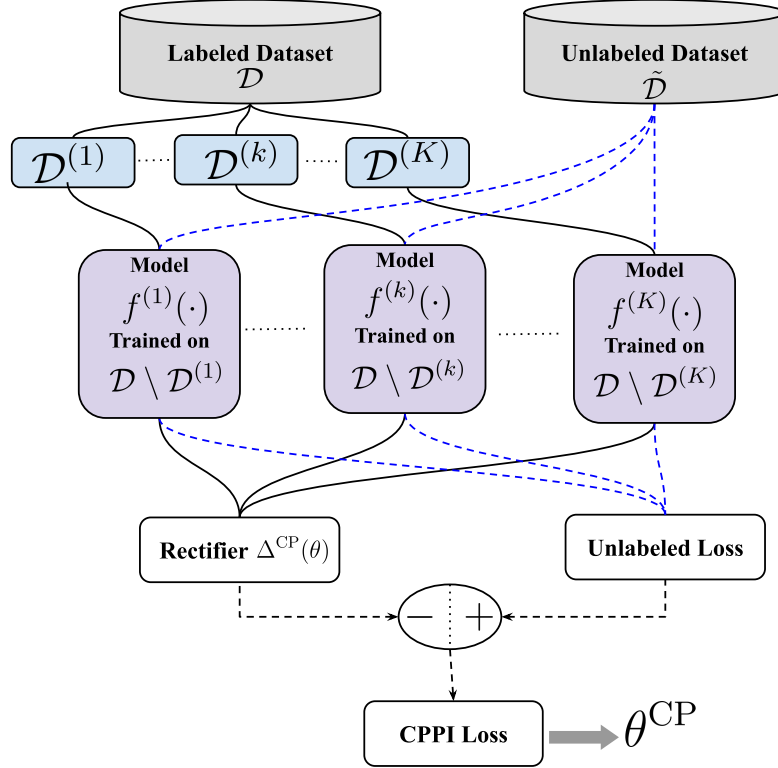


Fig. 2. Illustration of the CPPI scheme [22]: The labeled data is divided into K folds $\mathcal{D}^{(1)}, \dots, \mathcal{D}^{(K)}$, and K prediction models are trained, with each model $f^{(k)}(\cdot)$ being trained on all labeled data except for fold $\mathcal{D}^{(k)}$. Using the K trained models, a rectifier $\Delta^{\text{CP}}(\theta) = \frac{1}{n} \sum_{k=1}^K \sum_{i \in \mathcal{D}^{(k)}} [\ell_\theta(X_i, f^{(k)}(X_i)) - \ell_\theta(X_i, Y_i)]$ is evaluated that estimates the prediction bias of models $\{f^{(k)}(\cdot)\}_{k=1}^K$. This term is subtracted from the unlabeled loss $\frac{1}{KN} \sum_{k=1}^K \sum_{i=1}^N \ell_\theta(\tilde{X}_i, f^{(k)}(\tilde{X}_i))$, obtaining the CPPI loss $L^{\text{CP}}(\theta)$ in (2).

To this end, as illustrated in Fig. 2, CPPI operates in a way similar to cross-validation techniques [24]–[27]. Accordingly, K models $\{f^{(k)}(X)\}_{k=1}^K$ are trained using the labeled dataset, which are then used to annotate the unlabeled data and to obtain a rectifier for the prediction bias $\Delta^{\text{CP}}(\theta)$. This correction term is subtracted from the estimated loss $\frac{1}{KN} \sum_{k=1}^K \sum_{i=1}^N \ell_\theta(\tilde{X}_i, f^{(k)}(\tilde{X}_i))$ to obtain the estimate

$$L^{\text{CP}}(\theta) = \frac{1}{KN} \sum_{k=1}^K \sum_{i=1}^N \ell_\theta(\tilde{X}_i, f^{(k)}(\tilde{X}_i)) - \Delta^{\text{CP}}(\theta). \quad (2)$$

In this work, we showcase application scenarios for the PPI framework in wireless systems. We also introduce a new version of CPPI, called tuned CPPI, that allows the flexibility to adapt the use of unlabeled data as a function of the quality of the trained prediction models $\{f^{(k)}(X)\}_{k=1}^K$.

B. Main Contributions

The objective of this work is twofold. First, we study the benefits and potential application scenarios of the PPI framework for wireless communication systems. To this end, we first review PPI, tuned PPI, and CPPI, and then study two use cases in wireless systems, namely beam-alignment [28], [29] and localization [6], [7], [30]. Second, we propose a new variant of CPPI, referred to as tuned CPPI, that endows CPPI with the ability to adapt the use of unlabeled data to the quality of the ML prediction models, and thus to the amount of available labeled data.

To demonstrate the potential benefits of PPI and of the proposed tuned CPPI scheme for wireless systems, we study two application scenarios in which unlabeled data are more accessible than labeled data. As illustrated in Fig. 3(a), the first use case is beam alignment in millimeter-wave (mmWave) massive MIMO systems via channel knowledge maps (CKMs) [28], [29], [31]. Beam alignment requires selecting the index Y of the optimal beams within predefined codebooks given the location X of the device being served. CKMs represent site-specific databases containing channel information at given locations of receivers and transmitters, such as channel state information (CSI) matrices or partial information regarding the strongest signal paths [28], [29]. By leveraging a CKM, one can thus produce an estimate $f(\tilde{X})$ of the optimal beam for an unlabeled location \tilde{X} . The synthetic data $(\tilde{X}, f(\tilde{X}))$ can augment the labeled dataset (X, Y) of locations X and optimal beam indices Y . In this application, PPI and its extensions can be useful to correct the inevitable errors in the CSI provided by a CKM.

As a second application scenario, as shown in Fig. 3(b), we consider received signal strength information (RSSI)-based indoor localization. In RSSI-based positioning, RSSI measurements X at a number of access points (APs) are used to infer position Y of a mobile user [6], [30]. The accuracy of this positioning technique depends on the size of the available labeled dataset of pairs (X, Y) of RSSI fingerprint X and location Y . Additional unlabeled data consisting of RSSI measurements \tilde{X} was shown to be potentially useful by using semi-supervised learning [10], [11], [32]. PPI schemes can be thus beneficial as means to further enhance the reliability of semi-supervised learning in this context.

To summarize, the main contributions of this work are outlined as follows.

- We showcase applications of the PPI framework in wireless communication systems for scenarios in which acquiring labeled data is costly, presenting PPI as an alternative to conventional semi-supervised learning. Specifically, we highlight beam alignment via CKM

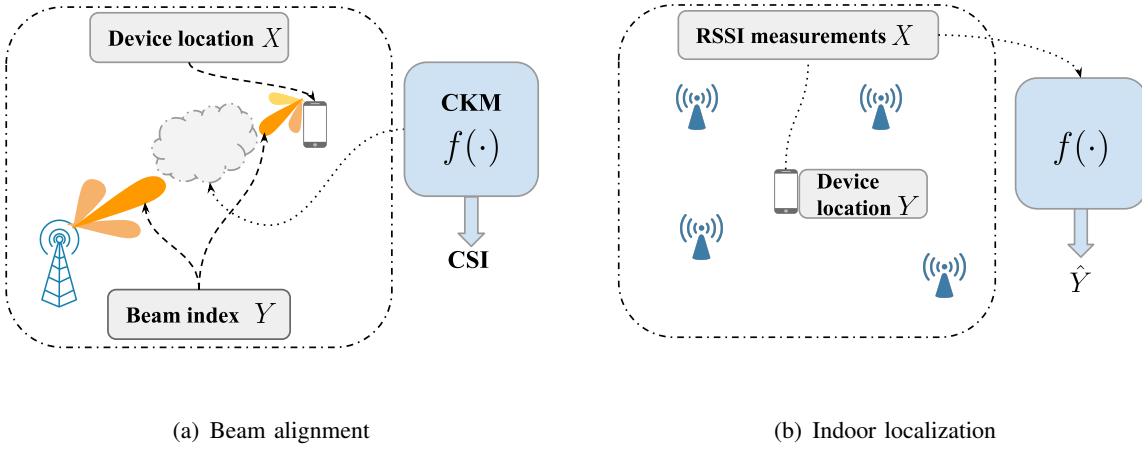


Fig. 3. Illustration of the two application scenarios: (a) beam alignment in mmWave communication systems, in which the optimal beam index Y is determined based on the device location X ; and (b) an indoor localization system based on RSSI, in which the position of the device Y is predicted based on RSSI measurements X received from access points. In both cases, a pre-trained ML model $f(\cdot)$ can be used to augment the labeled datasets, with a channel knowledge map (CKM) adopted for beam alignment.

and RSSI-based indoor localization as use cases.

- We introduce tuned CPPI, a novel extension of CPPI [22] that flexibly adapts the degree of reliance on unlabeled data depending on the quality of the ML-based predicted labels.
- The performance of the proposed tuned CPPI and existing PPI benchmarks is tested for the mentioned use cases, as well as for mean estimation and linear regression problems. Numerical results demonstrate the superiority of the proposed scheme over all the benchmark schemes, including conventional semi-supervised learning.

C. Organization

The rest of the paper is structured as follows. The next section introduces the semi-supervised setting and defines the studied problem. In Section III, we describe the PPI framework including its three variants, namely PPI, tuned PPI, and CPPI. In Section IV, the proposed tuned CPPI scheme is introduced. Section V provides simulation examples using synthetic data. Two applications to wireless systems, namely beam alignment for mmWave communication and RSSI-based indoor localization, are discussed in Sections VI and VII, respectively. Concluding remarks are drawn in Section VIII.

D. Notations

Given a vector x , x^T and x^H denote the transpose and conjugate of x . The trace of a matrix X is denoted by $\text{tr}(X)$. $|\mathcal{S}|$ is used to denote the cardinality of set \mathcal{S} . $\text{Var}(X)$ denotes the covariance matrix a random vector X , i.e., $\text{Var}(X) = \mathbb{E}[(X - \mathbb{E}[X])(X - \mathbb{E}[X])^T]$; while for random vectors X and Y , $\text{Cov}(X, Y)$ denotes the cross-covariance matrix, i.e., $\text{Cov}(X, Y) = \mathbb{E}[(X - \mathbb{E}[X])(Y - \mathbb{E}[Y])^T]$. For a sequence of random variables, $\{X_n\}_{n \in \mathbb{N}}$, we denote by $X_n \xrightarrow{P} X$ (resp. $X_n \xrightarrow{d} X$) the convergence in probability (resp. in distribution) to the random variable X in the limit $n \rightarrow \infty$.

II. PROBLEM DEFINITION

Consider a scenario in which acquiring high-quality labeled data is costly, while unlabeled samples are abundant. Specifically, a *labeled* dataset $\mathcal{D} = \{(X_i, Y_i)\}_{i=1}^n$ of n independent and identically distributed (i.i.d.) samples from an unknown distribution $P_{XY} = P_X \times P_{Y|X}$ is available, along with an *unlabeled* dataset $\tilde{\mathcal{D}} = \{\tilde{X}_i\}_{i=1}^N$ of N i.i.d. samples drawn from the marginal distribution P_X . The unlabeled dataset is typically much larger than the labeled dataset, i.e., $N \gg n$. Examples of this setting include medical applications requiring experts' annotations [33], [34] and engineering applications, such as wireless systems, in which labels may require the execution of costly optimizations on real-world data [2], [11], [16], [32].

Given a *convex* loss function $\ell_\theta(X, Y)$, the objective is to reliably estimate the minimizer $\theta^* \in \mathbb{R}^d$ of the *population loss* $L(\theta)$, i.e.,

$$\theta^* = \arg \min_{\theta} L(\theta), \quad \text{with } L(\theta) = \mathbb{E}[\ell_\theta(X, Y)], \quad (3)$$

where the expected value is taken over the unknown joint distribution P_{XY} . The formulation in (3) encompasses for instance mean estimation, quantile regression, and generalized linear models.

An unbiased estimator of the population loss in (3) can be obtained by using only the labeled data, yielding the classical *empirical risk minimization* (ERM) estimator

$$\theta^{\text{ERM}} = \arg \min_{\theta} L^{\text{ERM}}(\theta), \quad \text{with } L^{\text{ERM}}(\theta) = \frac{1}{n} \sum_{i=1}^n \ell_\theta(X_i, Y_i). \quad (4)$$

However, the ERM solution θ^{ERM} can have a high variance when the labeled dataset is of limited size. It is thus of interest to leverage also the unlabeled data in order to obtain a better estimate for the population-optimal parameter θ^* .

To this end, assume the availability of a *model* $f(X)$ that provides an estimate of the label Y . The model $f(X)$ can be a pretrained ML model or any other given predictor. Conventional *semi-supervised learning* addresses the problem [35]

$$\theta^{\text{SS}} = \arg \min_{\theta} L^{\text{SS}}(\theta), \quad \text{with} \quad L^{\text{SS}}(\theta) = \frac{n}{n+N} L^{\text{ERM}}(\theta) + \frac{\gamma}{n+N} \sum_{i=1}^N \ell_{\theta}(\tilde{X}_i, f(\tilde{X}_i)), \quad (5)$$

where the loss $L^{\text{SS}}(\theta)$ averages over both labeled and unlabeled data, and $\gamma \geq 0$ is a hyperparameter dictating the confidence in the synthetic labels [16], [35], [36]. Note that with $\gamma = 1$ synthetic and real labels are treated on an equal footing.

Accordingly, conventional semi-supervised learning optimizes a biased estimate of the population loss in (3), and the bias may cause significant performance degradation when the model $f(X)$ is not sufficiently accurate [18], [21], [22].

III. PREDICTION-POWERED INFERENCE

Prediction-powered inference (PPI) [18] and its variants [21], [22] provide principled alternatives to the conventional semi-supervised estimator (5), which have been shown to have the desirable theoretical guarantees and empirical performance. This section reviews PPI [18], tuned PPI [21], and cross-PPI [22], providing the necessary background for the introduction of tuned cross-PPI in the next section.

A. Prediction-Powered Inference

In the setting described in the previous section, PPI uses the labeled data to quantify, and compensate for, the prediction bias of the model $f(X)$ as compared to the ground-truth labels. To this end, PPI addresses the problem [18]

$$\theta^{\text{PP}} = \arg \min_{\theta} L^{\text{PP}}(\theta), \quad (6)$$

with cost function

$$L^{\text{PP}}(\theta) = \frac{1}{N} \sum_{i=1}^N \ell_{\theta}(\tilde{X}_i, f(\tilde{X}_i)) - \left[\frac{1}{n} \sum_{i=1}^n \ell_{\theta}(X_i, f(X_i)) - L^{\text{ERM}}(\theta) \right]. \quad (7)$$

Unlike the conventional estimate $L^{\text{SS}}(\theta)$ in (5), the loss function $L^{\text{PP}}(\theta)$ is an *unbiased* estimate of the population loss $L(\theta)$ in (3). In fact, the expected values of the first and second terms in (7) are equal, canceling each other.

The intuition behind the loss function (7) is that the term in the square brackets serves as a *rectifier* for the bias caused by the use of the model $f(X)$ to assign labels in the unlabeled loss $\sum_{i=1}^N \ell_\theta(\tilde{X}_i, f(\tilde{X}_i))/N$. In fact, the rectifier term measures the error in the estimate of the loss on the labeled data points. The PPI objective (7) subtracts the estimated error from the unlabeled loss, making the loss estimate (7) unbiased.

Under the assumption that the loss function $\ell_\theta(X, Y)$ is a convex function of parameter θ , reference [18] demonstrated that the variance of the estimate $\hat{\theta}^{\text{PP}}$ is lower than that of the ERM estimator (4) as long as the model $f(X)$ is sufficiently accurate. Reference [18] also provided confidence sets for the optimal solution θ^* using the PPI estimate (6).

B. Tuned Prediction-Powered Inference

PPI is not guaranteed to improve over ERM when the model $f(X)$ is not sufficiently accurate. To address this issue, reference [21] proposed *tuned PPI*, a variant of PPI that automatically adapts to the quality of the prediction model $f(X)$. Tuned PPI selects the parameter vector θ as

$$\theta_\lambda^{\text{PP}} = \arg \min_{\theta} L_\lambda^{\text{PP}}(\theta), \quad (8)$$

where the cost function is defined as

$$L_\lambda^{\text{PP}}(\theta) = L^{\text{ERM}}(\theta) + \lambda \left[\frac{1}{N} \sum_{i=1}^N \ell_\theta(\tilde{X}_i, f(\tilde{X}_i)) - \frac{1}{n} \sum_{i=1}^n \ell_\theta(X_i, f(X_i)) \right], \quad (9)$$

and $\lambda \in [0, 1]$ is a tuning parameter.

As for PPI, the loss in (9) is an unbiased estimate of the population loss $L(\theta)$ for any value $\lambda \in [0, 1]$. By varying parameter λ , tuned PPI ranges from ERM, which is obtained for $\lambda = 0$, to PPI, which is recovered for $\lambda = 1$. Reference [21] proposed a procedure to set the parameter λ with the aim of minimizing the variance of the estimate $\theta_\lambda^{\text{PP}}$. This way, when the predictor $f(X)$ is inaccurate, tuned PPI can revert to the conventional ERM estimator by setting $\lambda = 0$ in (9).

C. Cross-Prediction-Powered Inference

PPI and tuned PPI assume the availability of a model $f(X)$. In practice, however, model $f(X)$ may have to be trained using labeled data. Therefore, the available labeled dataset must be shared between the task of obtaining the prediction model $f(X)$ and the task of estimating the parameter vector θ using (6) or (8).

Cross-PPI (CPPI) addresses this problem via *cross-validation*, enabling the use of the entire labeled dataset for training model $f(X)$, as well as for estimating parameter θ . As in cross-validation, the labeled dataset $\mathcal{D} = \{(X_i, Y_i)\}_{i=1}^n$ is divided into K *folds*, with the first fold including data points (X_i, Y_i) with indices i in $\mathcal{D}^{(1)} = \{1, \dots, n/K\}$, the second fold including data points (X_i, Y_i) with indices i in $\mathcal{D}^{(2)} = \{n/K + 1, \dots, 2n/K\}$, and so on for the other folds $\mathcal{D}^{(3)}, \dots, \mathcal{D}^{(K)}$. For each $k = 1, \dots, K$, a model $f^{(k)}(X)$ is trained on all folds except for fold $\mathcal{D}^{(k)}$. As detailed next, the predictions of the K models $\{f^{(k)}(X)\}_{k=1}^K$ are used to estimate the parameter vector θ^* based on both labeled and unlabeled data.

Specifically, the cross-PPI estimate is obtained as

$$\theta^{\text{CP}} = \arg \min_{\theta} L^{\text{CP}}(\theta), \quad (10)$$

with cost function

$$L^{\text{CP}}(\theta) = \frac{1}{KN} \sum_{k=1}^K \sum_{i=1}^N \ell_{\theta}(\tilde{X}_i, f^{(k)}(\tilde{X}_i)) - \left[\frac{1}{n} \sum_{k=1}^K \sum_{i \in \mathcal{D}^{(k)}} \ell_{\theta}(X_i, f^{(k)}(X_i)) - L^{\text{ERM}}(\theta) \right]. \quad (11)$$

The first term in (11) is the empirical loss that uses the predictions of the K models on the unlabeled data, while the second, rectifier, term corrects the bias caused by the use of the trained models $\{f^{(k)}(X)\}_{k=1}^K$ in the first term. In this regard, note that the correction term for model $f^{(k)}(X)$ in (11) is obtained by using data in fold $\mathcal{D}^{(k)}$, which is independent of the data model $f^{(k)}(X)$ was trained on. As a result, the CPPI loss $L^{\text{CP}}(\theta)$ is an unbiased estimate of the population loss $L(\theta)$.

IV. TUNED CROSS-PREDICTION-POWERED INFERENCE

The quality of the CPPI estimate (10) depends on the accuracy of the trained models $\{f^{(k)}(X)\}_{k=1}^K$ in (11). Therefore, when the trained models are not sufficiently accurate, CPPI is not guaranteed to improve over ERM, which uses only labeled data. Inspired by tuned PPI, in this section we introduce *tuned CPPI*, which provides the flexibility to judiciously adapt the use of unlabeled data as a function of the quality of the trained models $\{f^{(k)}(X)\}_{k=1}^K$.

A. Tuned Cross-Prediction-Powered Inference

In a manner similar to the tuned CPPI loss in (13), tuned CPPI introduces a tuning parameter λ in the CPPI loss (11) so as to determine the degree of reliance on the unlabeled data depending

on the quality of the trained models. Specifically, the proposed tuned CPPI estimator is given by

$$\theta_\lambda^{\text{CP}} = \arg \min_{\theta} L_\lambda^{\text{CP}}(\theta), \quad (12)$$

where the loss function is

$$L_\lambda^{\text{CP}}(\theta) = L^{\text{ERM}}(\theta) + \lambda \left[\frac{1}{KN} \sum_{k=1}^K \sum_{i=1}^N \ell_\theta(\tilde{X}_i, f^{(k)}(\tilde{X}_i)) - \frac{1}{n} \sum_{k=1}^K \sum_{i \in \mathcal{D}^{(k)}} \ell_\theta(X_i, f^{(k)}(X_i)) \right]. \quad (13)$$

The tuned CPPI loss $L_\lambda^{\text{CP}}(\theta)$ reduces to the CPPI loss in (11) when $\lambda = 1$ and it recovers the ERM loss (4) when $\lambda = 0$.

As for CPPI and ERM, the tuned CPPI loss in (13) is an unbiased estimate of the population loss $L(\theta)$ for any $\lambda \in [0, 1]$, i.e.,

$$\mathbb{E}[L_\lambda^{\text{CP}}(\theta)] = L(\theta), \quad (14)$$

where the average is taken over labeled and unlabeled data. Unlike CPPI, tuned CPPI offers the flexibility to tune the parameter $\lambda \in [0, 1]$ as a function of the quality of the trained models. This is done with the aim of minimizing the mean squared error (MSE) of the estimate $\theta_\lambda^{\text{CP}}$ in (12). That is, the parameter λ is ideally chosen as the minimizer

$$\lambda^* = \arg \min_{\lambda} \text{MSE}(\lambda), \text{ with } \text{MSE}(\lambda) = \mathbb{E}[\|\theta_\lambda^{\text{CP}} - \theta^*\|_2^2], \quad (15)$$

with average evaluated over labeled and unlabeled data. The MSE in (15) is estimated in practice from the data, yielding a data-dependent estimate $\hat{\lambda}_n$ of the ideal tuning parameter λ^* . To this end, the next section derives an explicit expression for the optimal parameter λ^* , which is then approximated by using data to obtain the estimate $\hat{\lambda}_n$.

B. Optimal Tuning Parameter

In this subsection, we aim at deriving an explicit expression for the optimal tuning parameter λ^* in (15). To start, we note that the trained models $\{f^{(k)}(X)\}_{k=1}^K$ are identically distributed, since they are trained on identically distributed data. Define the average predictor as

$$\bar{f}(\cdot) = \mathbb{E}[f^{(1)}(\cdot)] = \dots = \mathbb{E}[f^{(K)}(\cdot)], \quad (16)$$

where the expectation is taken over the labeled data used to train the models $\{f^{(k)}(X)\}_{k=1}^K$. The average model $\bar{f}(x)$ can be interpreted as the predictor obtained by training many models on

independent datasets of size $n - n/K$, and then averaging their predictions. The analysis of the mean squared error $\text{MSE}(\lambda)$ in (15) is based on the following assumption, which formalizes the property that the gradient of the population loss $\nabla \ell_\theta(X, f^{(k)}(X))$ does not depend too strongly on the model index k as the number of labeled data points, n , increases.

Assumption 1. *For input $X \sim P_X$ independent of model $f^{(k)}(\cdot)$, denote by $\text{Var}(\nabla \ell_\theta(X, f^{(k)}(X)) - \nabla \ell_\theta(X, \bar{f}(X))|f^{(k)})$ the covariance matrix of the random vector $\nabla \ell_\theta(X, f^{(k)}(X)) - \nabla \ell_\theta(X, \bar{f}(X))$ for a fixed model $f^{(k)}(\cdot)$. The square root of the entries of $\text{Var}(\nabla \ell_\theta(X, f^{(k)}(X)) - \nabla \ell_\theta(X, \bar{f}(X))|f^{(k)})$ are assumed to converge in mean to zero, i.e.,*

$$\mathbb{E} \left[\sqrt{\text{Var}(\nabla \ell_\theta(X, f^{(k)}(X)) - \nabla \ell_\theta(X, \bar{f}(X))|f^{(k)})} \right] \xrightarrow{n \rightarrow \infty} 0, \quad \text{for any } k \in \{1, \dots, K\}, \quad (17)$$

where the outer expectation is taken over the distribution of the model $f^{(k)}(\cdot)$. The square root and the convergence in (17) are applied entry-wise.

Generalizing [22, Theorem 2] and [21, Theorem 1], the following theorem establishes the asymptotic normality of the tuned CPPI estimator $\hat{\theta}_\lambda^{\text{CP}}$ in (12). This result will be then used to evaluate the optimal tuning parameter λ^* in (15). To simplify notations, we define the Hessian of the population loss as $H_\theta = \nabla^2 L(\theta)$; we let $\nabla \ell_\theta = \nabla \ell_\theta(X, Y)$ be the gradient of the loss on a labeled data point (X, Y) ; and we write $\nabla \ell_{\theta}^{\bar{f}} = \nabla \ell_\theta(X, \bar{f}(X))$ for the gradient of the loss on a data point X with label assigned by the average model $\bar{f}(\cdot)$ in (16). Furthermore, we denote as

$$V_{\bar{f}, \theta^*}^\lambda = \lambda^2 \text{Var} \left(\nabla \ell_{\theta^*}^{\bar{f}} \right) \quad (18)$$

the covariance matrix of the gradient $\nabla \ell_{\theta^*}^{\bar{f}}$, and as

$$V_{\Delta, \theta^*}^\lambda = \text{Var} \left(\nabla \ell_{\theta^*} - \lambda \nabla \ell_{\theta^*}^{\bar{f}} \right) \quad (19)$$

the covariance matrix of $\nabla \ell_{\theta^*} - \lambda \nabla \ell_{\theta^*}^{\bar{f}}$.

Theorem 1. *For $n \rightarrow \infty$ with $n/N = r$, assume that the estimate $\hat{\lambda}_n$ converges to some value λ , i.e., $\hat{\lambda}_n \xrightarrow{P} \lambda$, and that the corresponding parameter $\theta_{\hat{\lambda}_n}^{\text{CP}}$ in (12) converges to the optimal value θ^* , i.e., $\theta_{\hat{\lambda}_n}^{\text{CP}} \xrightarrow{P} \theta^*$. Then, we have the limit*

$$\sqrt{n}(\theta_{\hat{\lambda}_n}^{\text{CP}} - \theta^*) \xrightarrow[n \rightarrow \infty]{d} \mathcal{N}(0, \Sigma_\lambda), \quad (20)$$

with covariance matrix

$$\Sigma_\lambda = H_{\theta^*}^{-1} \left(r \cdot V_{\bar{f}, \theta^*}^\lambda + V_{\Delta, \theta^*}^\lambda \right) H_{\theta^*}^{-1}. \quad (21)$$

Proof. The proof follows the same techniques used in [22, Theorem 2] and [21, Theorem 1], and is thus omitted. \square

We note that for a fixed $\lambda \in [0, 1]$, the consistency $\theta_\lambda^{\text{CP}} \xrightarrow{P} \theta^*$ holds if the loss function $L_\lambda^{\text{CP}}(\theta)$ is convex in θ or the parameter space is compact [18], [21], [22], [37]. For instance, the convexity of loss $L_\lambda^{\text{CP}}(\theta)$ holds for all generalized linear models. We refer the reader to [21], [37] for more discussion.

By (20), the asymptotic mean squared error, which is proportional to $\text{tr}(\Sigma_\lambda)$, depends on the curvature of the population loss around the optimal value θ^* via the Hessian H_{θ^*} ; on the inherent variability of the average predictor $\bar{f}(X)$ via the term $V_{\bar{f}, \theta^*}^\lambda$ in (18); and on the accuracy of the average predictor $\bar{f}(X)$ via the term $V_{\Delta, \theta^*}^\lambda$ in (19).

With this result at hand, the optimal tuning parameter λ^* in (15) can be evaluated, in the limit $n \rightarrow \infty$, as

$$\lambda^* = \arg \min_\lambda \text{tr}(\Sigma_\lambda) = \frac{\text{tr} \left(H_{\theta^*}^{-1} \left(\text{Cov}(\nabla \ell_{\theta^*}, \nabla \ell_{\theta^*}^{\bar{f}}) + \text{Cov}(\nabla \ell_{\theta^*}^{\bar{f}}, \nabla \ell_{\theta^*}) \right) H_{\theta^*}^{-1} \right)}{2(1+r) \text{tr} \left(H_{\theta^*}^{-1} \text{Var}(\nabla \ell_{\theta^*}^{\bar{f}}) H_{\theta^*}^{-1} \right)}, \quad (22)$$

where $\text{Cov}(\nabla \ell_{\theta^*}, \nabla \ell_{\theta^*}^{\bar{f}})$ represent the cross-covariance matrix of vectors $\nabla \ell_{\theta^*}$ and $\nabla \ell_{\theta^*}^{\bar{f}}$ with respect to random variables $(X, Y) \sim P_{XY}$; and $\text{Var}(\nabla \ell_{\theta^*}^{\bar{f}})$ is the covariance matrix of vector $\nabla \ell_{\theta^*}^{\bar{f}}$ with respect to random variable $X \sim P_X$. To estimate the optimal parameter λ^* in practice, we resort to bootstrapping techniques, as done in [22] for estimating the variance of the CPPI estimator. This is described next.

C. Estimating the Optimal Tuning Parameter

The optimized tuning parameter λ^* in (22) requires the evaluation of the Hessian H_{θ^*} , of the covariance matrix $\text{Var}(\nabla \ell_{\theta^*}^{\bar{f}})$ of vector $\nabla \ell_{\theta^*}^{\bar{f}}$, and of the cross-covariance matrix $\text{Cov}(\nabla \ell_{\theta^*}, \nabla \ell_{\theta^*}^{\bar{f}})$ between vectors $\nabla \ell_{\theta^*}$ and $\nabla \ell_{\theta^*}^{\bar{f}}$. These quantities depend on the optimal parameter vector θ^* and on the average predictor $\bar{f}(X)$ in (16), and they need to be estimated from data. To this end, as in [21], we first fix an arbitrary value $\lambda \in [0, 1]$ to obtain an estimate of the optimal parameter vector θ^* via the solution $\theta_\lambda^{\text{CP}}$ in (12). This estimate, which we denote as $\hat{\theta}$, is consistent for

convex loss functions $L_\lambda^{\text{CP}}(\theta)$, as discussed in Sec. IV-B. The Hessian H_{θ^*} is then estimated by using the empirical estimate

$$\hat{H}_{\hat{\theta}} = \frac{1}{n} \sum_{i=1}^n \nabla^2 \ell_{\hat{\theta}}(X_i, Y_i), \quad (23)$$

obtained from the labeled data.

Then, as in [22], we apply bootstrapping to simulate several runs of the training process, obtaining an estimate of the average predictor $\bar{f}(X)$. The estimates of $\text{Var}(\nabla \ell_{\theta^*})$ and $\text{Cov}(\nabla \ell_{\theta^*}, \nabla \ell_{\theta^*})$, denoted by $\widehat{\text{Var}}(\nabla \ell_{\theta^*})$ and $\widehat{\text{Cov}}(\nabla \ell_{\theta^*}, \nabla \ell_{\theta^*})$, respectively, are obtained by using empirical estimates from labeled and unlabeled data as detailed in the appendix.

Using the estimates $\hat{H}_{\hat{\theta}}$, $\widehat{\text{Var}}(\nabla \ell_{\hat{\theta}})$, and $\widehat{\text{Cov}}(\nabla \ell_{\hat{\theta}}, \nabla \ell_{\hat{\theta}})$, a plug-in estimator of the optimal parameter λ^* in (22) is finally obtained as

$$\hat{\lambda} = \frac{\text{tr} \left(\hat{H}_{\hat{\theta}}^{-1} \left(\widehat{\text{Cov}}(\nabla \ell_{\hat{\theta}}, \nabla \ell_{\hat{\theta}}) + \widehat{\text{Cov}}(\nabla \ell_{\hat{\theta}}^T, \nabla \ell_{\hat{\theta}}) \right) \hat{H}_{\hat{\theta}}^{-1} \right)}{2(1+n/N) \text{tr} \left(\hat{H}_{\hat{\theta}}^{-1} \widehat{\text{Var}}(\nabla \ell_{\hat{\theta}}) \hat{H}_{\hat{\theta}}^{-1} \right)}. \quad (24)$$

The optimized parameter $\hat{\lambda}$ in (24) can fall outside the interval $[0, 1]$. To solve this issue, one can clip its value back to $[0, 1]$ or apply one-step estimators [21], [37]. We adopt the first option in our experiments.

Overall, obtaining the estimate $\hat{\lambda}$ in (24) involves two main steps. First, an estimate $\hat{\theta}$ of the optimal parameter θ^* is obtained by addressing problem (12) for a fixed $\lambda \in [0, 1]$, and parameter $\hat{\lambda}$ is computed using (24). Then, the tuned CPPI estimator is obtained by addressing problem (12) using $\lambda = \hat{\lambda}$. Algorithm 1 outlines the key steps of the proposed scheme.

Finally, we note that for the case of mean estimation, where the objective is to estimate parameter $\theta = \mathbb{E}[Y]$ and the loss function in (3) corresponds to $\ell_\theta(X, Y) = (Y - \theta)^2$, the optimal tuning parameter λ^* in (22) has the simplified expression [21]

$$\lambda^* = \frac{\text{Cov}(Y, \bar{f}(X))}{(1+r) \text{Var}(\bar{f}(X))}, \quad (25)$$

which can be estimated in a manner analogous to (24).

V. MEAN ESTIMATION AND LINEAR REGRESSION

In this section, we report the results of an experiment using synthetic data to provide a first performance comparison across all PPI schemes. Specifically, we consider two variants of the estimation problem in (3), namely mean estimation, corresponding to the loss function $\ell_\theta(X, Y) = (Y - \theta)^2$ with $Y \in \mathbb{R}$ and $\theta \in \mathbb{R}$, and linear regression coefficients estimation,

Algorithm 1: Tuned CPPI

Input: Labeled dataset \mathcal{D} , unlabeled dataset $\tilde{\mathcal{D}}$, number of prediction models K

Output: Tuned CPPI parameter estimate

- 1 Use the labeled data to train the prediction models $\{f^{(k)}(X)\}_{k=1}^K$ using the procedure described in Section III-C
 - 2 Fix $\lambda_1 \in [0, 1]$
 - 3 Compute the tuned CPPI loss in (13) for $\lambda = \lambda_1$ using the labeled and unlabeled data and solve (12) to obtain $\hat{\theta} = \theta_{\lambda_1}^{\text{CP}}$
 - 4 Compute the Hessian estimate $\hat{H}_{\hat{\theta}}$ using (23)
 - 5 Compute $\widehat{\text{Var}}(\nabla \ell_{\theta^*})$ and $\widehat{\text{Cov}}(\nabla \ell_{\theta^*}, \nabla \ell_{\theta^*}^T)$ using (37) and (38), respectively
 - 6 Obtain $\hat{\lambda}_n$ using (24)
 - 7 Solve (12) again for $\lambda = \hat{\lambda}_n$ to obtain $\theta_{\hat{\lambda}_n}^{\text{CP}}$
-

corresponding to the loss function $\ell_{\theta}(X, Y) = (Y - X^T \theta)^2$ with $X \in \mathbb{R}^d$, $Y \in \mathbb{R}$, and $\theta \in \mathbb{R}^d$. In all experiments in this section, we fix the size of the unlabeled dataset to $N = 10000$ samples, and we vary the size of the unlabeled dataset n .

We consider the following model for data generation as in [22]

$$Y = \mu + X^T \beta + z, \quad (26)$$

where $\mu \in \mathbb{R}$ is a fixed constant, $X \in \mathbb{R}^d$ is distributed as $X \sim \mathcal{N}(0, I_d)$, $\beta = \frac{R\sigma}{\sqrt{2}}[1, \dots, 1]^T \in \mathbb{R}^d$ for some given positive constants R and σ , and $z \sim \mathcal{N}(0, \sigma^2(1 - R^2))$ is independent of X . Parameters μ and σ are fixed in all experiments, while parameter R is varied in the interval $[0, 1]$. Parameter R dictates the degree to which the output variable Y can be explained through the feature vector X . In particular, when $R = 0$, the label Y is independent of X , while, when $R = 1$, the label Y is a deterministic function of X .

For the CPPI and tuned CPPI schemes, $K = 5$ models are trained by following the cross-validation procedure in Sec. III-C, where each model $f^{(k)}(X)$ is a random forest regression model [38]. For the PPI and tuned PPI schemes, as in [22], half of the labeled data is used to train a random forest regression model $f(X)$, and the rest is used for estimating θ . The MSE between the true parameter vector and its estimate is used as a performance metric. We compare the performance of the proposed tuned CPPI scheme with the benchmark schemes ERM, SS

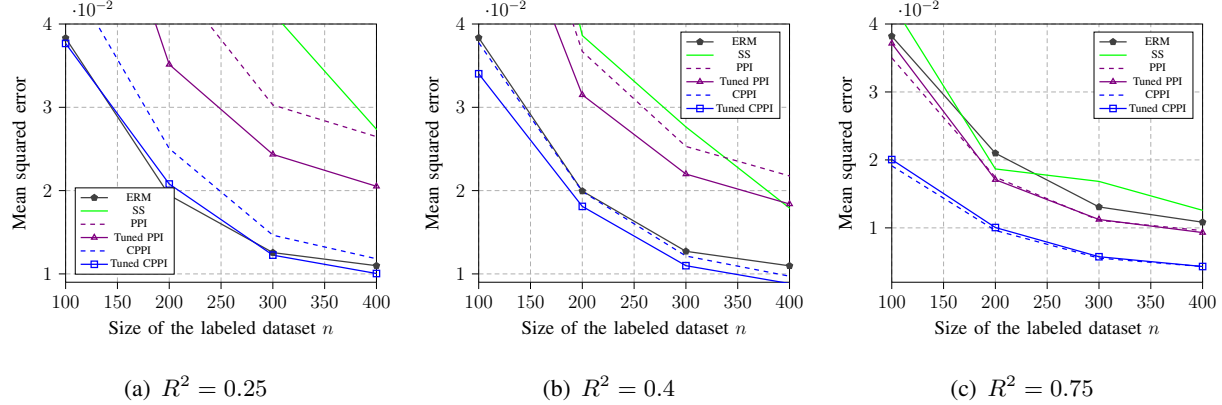


Fig. 4. Mean squared error as a function of the size of the labeled dataset for the problem of men estimation under the synthetic data-generation model (26). The results are averaged over 300 trials.

(with $\gamma = 1$), PPI, tuned PPI, and CPPI described in Sec. II and in Sec. III.

A. Mean Estimation

Given the data generation model in (26), the target here is the mean of variable Y , i.e., $\theta^* = \mathbb{E}[Y] = \mu$. Here, we fix $d = 2$, $\sigma = 2$, and $\mu = 4$. Fig. 4 shows the performance of all schemes versus the number of data points in the labeled dataset, n , for different values of the correlation parameter R . The performance is measured in terms of the MSE between the true mean μ and its estimate. The proposed tuned CPPI guarantees the best performance under all settings. Specifically, when R is small (Fig. 4(a)), here $R^2 = 0.25$, which implies a low dependence of Y on the feature vector X , tuned CPPI performs close to ERM, while outperforming CPPI, as the trained models are not expected to help in this case. Conversely, for high values of R (Fig. 4(c)), here $R^2 = 0.75$, tuned CPPI and CPPI have comparable performance and significantly outperform ERM. In the intermediate regime, corresponding to $R^2 = 0.4$, tuned CPPI outperforms both CPPI and ERM (Fig. 4(b)).

B. Linear Regression

Using the data generation model (26) with $d = 3$, $\mu = 0$, and $\sigma = 2$, we consider here estimating the coefficients of a linear regression model, following a standard feature selection

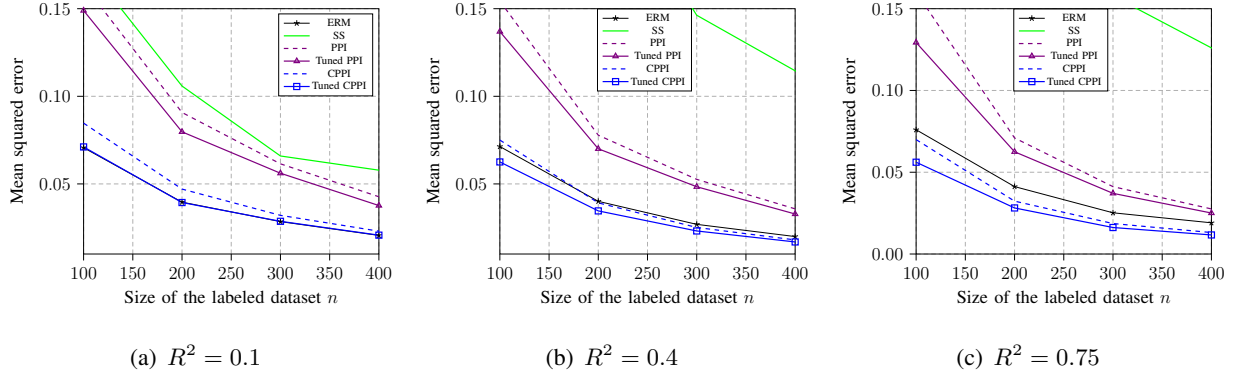


Fig. 5. Mean squared error as a function of the size of the labeled dataset for the problem of linear regression under the synthetic data-generation model (26). The results are averaged over 300 trials.

methodology [39], only the first two features (X_1, X_2) are included as covariates, that is, the target is the parameter vector $\theta^* \in \mathbb{R}^2$ given by

$$\theta^* = \arg \min_{\theta} \mathbb{E} [(Y - X_{\text{red}}^T \theta)^2], \quad (27)$$

where $X_{\text{red}} = [X_1, X_2]^T$. The performance metric is the MSE between the true parameter vector $\theta^* = [\beta_1, \beta_2]^T$ and its estimate.

We report in Fig. 5 the performance of all schemes versus the labeled dataset size n for different values of R . We observe a similar behavior as in the mean estimation case. In particular, tuned CPPI guarantees the best performance in all settings, yielding better results than CPPI for low values of R , outperforming ERM for high values of R , and improving over both schemes in the intermediate regime of parameter R . Moreover, we note that the SS scheme, which disregards the prediction bias of the trained models, demonstrates significantly inferior performance.

VI. PREDICTION-POWERED BEAM ALIGNMENT IN MMWAVE MASSIVE MIMO

Beamforming design is a crucial task in mmWave massive MIMO systems [40]–[42], as beamforming is necessary to compensate for the more severe path loss experienced at higher carrier frequencies [43]. Codebook-based beam alignment consists of selecting the best beam from codebooks of predefined beams based on beam sweeping, which requires transmission of pilot signals [41], [43].

Recently, a new approach has emerged that alleviates the training overhead by leveraging the concept of a channel knowledge map (CKM). As discussed in Sec. I, a CKM is a site-specific

database of channel information linked to transmitter and receiver locations [28], [29]. In this section, we propose a method that trains a mapping between a user's location and a pair of beams within their respective codebooks by leveraging both labeled and unlabeled data. As detailed below and illustrated in Fig. 3(a), labeled data consists of a user's location and the corresponding CSI, while unlabeled data only includes a user's location. Furthermore, for the unlabeled inputs X , CSI parameters are estimated using a CKM.

A. System Model

As in [28], [29], we consider a downlink mmWave massive MIMO communication system, in which a base station (BS) equipped with N^{TX} transmit antennas communicates with a user equipment (UE) with N^{RX} receive antennas. We assume that both BS and UE have a single radio frequency chain, and that beamforming is achieved using phase shifters in the analog domain. The beamforming vectors at the BS and the UE, denoted as $u \in \mathbb{C}^{N^{TX} \times 1}$ and $w \in \mathbb{C}^{N^{RX} \times 1}$, respectively, are ideally chosen from finite codebooks \mathcal{U} and \mathcal{W} by maximizing the signal-to-noise ratio (SNR). Indexing the set of all beamforming pairs $(u, w) \in \mathcal{U} \times \mathcal{W}$ as (u_j, w_j) with $j \in \mathcal{J} = \{1, \dots, J = |\mathcal{U}| |\mathcal{W}|\}$, the optimal beam index is obtained as

$$Y = \arg \max_{j \in \mathcal{J}} |u_j^H H w_j|^2, \quad (28)$$

where $H \in \mathbb{C}^{N^{TX} \times N^{RX}}$ is the current channel matrix. Accordingly, the ideal beam selection in (28) requires knowledge of the current channel matrix H .

When the current CSI is unknown, an alternative is to select the beams (u_j, w_j) based solely on the location $X \in \mathbb{R}^3$ of the UE [28]. To this end, we adopt here a softmax regression model that maps a feature vector $\psi(X) \in \mathbb{R}^m$ of the UE location X to the corresponding estimated beam index $\hat{Y} \in \mathcal{J}$. The feature vector $\psi(X)$ is obtained here using the radial basis function (RBF) kernel with Nyström approximation [44].

The beam index is then selected based on the location X as

$$\hat{Y} = \arg \max_{j \in \mathcal{J}} \left\{ \frac{\exp(\theta_j^T \psi(X))}{\sum_{j' \in \mathcal{J}} \exp(\theta_{j'}^T \psi(X))} \right\}, \quad (29)$$

where $\theta = [\theta_1^T, \dots, \theta_J^T]^T$, with $\theta_j \in \mathbb{R}^m$, is a parameter vector. The optimal beam selection parameter θ^* is obtained as the solution of the problem

$$\theta^* = \arg \min_{\theta} \mathbb{E}[\ell_{\theta}(X, Y)], \quad (30)$$

where the average is over the joint distribution of the UE location X and of the corresponding optimal beam Y in (28); and the loss function $\ell_\theta(X, Y)$ is the regularized softmax regression loss [45]

$$\ell_\theta(X, Y) = - \sum_{j \in \mathcal{J}} \mathbb{1}\{Y = j\} \log \frac{\exp(\theta_j^T \psi(X))}{\sum_{j' \in \mathcal{J}} \exp(\theta_{j'}^T \psi(X))} + \gamma \|\theta\|_2^2, \quad (31)$$

with $\gamma \geq 0$ being a regularization parameter. Problem (30) is in the form (3), since the loss $\ell_\theta(X, Y)$ is a convex function of parameters θ .

To address problem (30), we assume access to a labeled dataset $\mathcal{D} = \{(X_i, Y_i)\}_{i=1}^n$ where label Y is obtained from available CSI using (28), as well as an unlabeled dataset $\tilde{\mathcal{D}} = \{\tilde{X}_i\}_{i=1}^N$ drawn from the distribution P_X of the UE's locations. Note that prior information about the UE location distribution can be more easily acquired than CSI via passive tracking systems for instance [46], [47].

B. CKM-Based Beam Alignment

In order to use the unlabeled data of the user's locations, it is necessary to train a model $f(X)$ that maps UE location X to beam index Y . To this end, we consider a model of the form

$$Y = f(X) = g(c(X)), \quad (32)$$

where $c(X)$ is the CKM-based mapping between position X and CSI matrix H , while function $g(\cdot)$ maps CSI H to the optimal beam index by solving (28) with $H = c(X)$.

To define the CKM-based mapping function $c(X)$, we follow [29], which assigns to each position X multi-path information Z defined as

$$Z = \left\{ L, \{\alpha^l, \theta_{AoD}^l, \phi_{AoD}^l, \theta_{AoA}^l, \phi_{AoA}^l\}_{l=1}^L \right\}, \quad (33)$$

where L is the number of significant paths; α^l is the complex gain of the l -th path; θ_{AoA}^l and ϕ_{AoA}^l are the zenith and azimuth angles of arrival (AoA); and θ_{AoD}^l and ϕ_{AoD}^l are the zenith and azimuth angles of departure (AOD). From the path information Z , one can construct an estimate of the channel matrix H using a standard multipath model

$$H = h(Z). \quad (34)$$

In order to enable the training of the CKM function $H = c(X)$, and thus of the model $f(X)$ in (32), we assume access to a labeled dataset $\mathcal{D}_Z = \{X_i, Z_i\}_{i=1}^n$ containing pairs of UE locations X_i and the corresponding path information Z_i . Using the channel function (34) and the optimal beam index (28), one can recover the labeled data $\mathcal{D} = \{X_i, Y_i\}_{i=1}^n$.

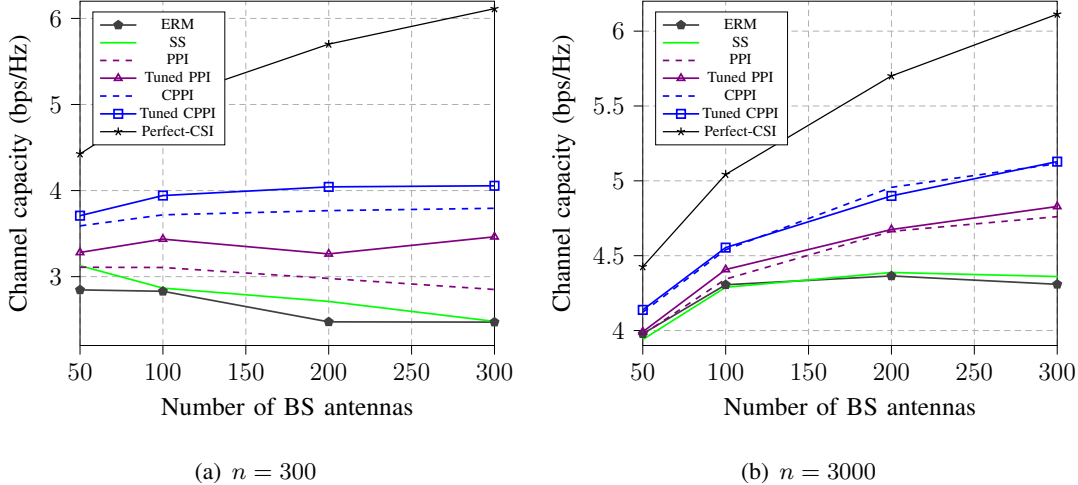


Fig. 6. Channel capacity as a function of the number of BS antennas for different values of the labeled dataset size n .

C. Numerical Results

We compare the performance of the proposed tuned CPPI approach to the benchmark schemes ERM, SS (with $\gamma = 1$), PPI, tuned PPI, and CPPI described in Sec. II and Sec. III. We also use as a reference the ideal case of perfect CSI. For CPPI and tuned CPPI, we train $K = 8$ models using the procedure described in Section III-C. As for PPI and tuned PPI, the labeled dataset is divided into two subsets of equal size, one used for training the prediction model $f(X)$ in (32), and the other for bias correction when computing the PPI and tuned PPI losses in (7) and (9), respectively. The PPI model $f(X)$ and the CPPI models $\{f^{(k)}(X)\}$ are obtained using (32), where the CKM function $c(X)$ is implemented as a fully connected neural network with three hidden layers of size 128, 256, and 1024, respectively, with the LeakyRelu activation function [48].

We consider the same physical environment and dataset as in [28]. The dataset contains ground-truth multi-path channel information Z in (33) generated by using the *ray tracing* software Remcom Wireless Insite¹. The BS is equipped with a uniform planar array (UPA), and the UE is equipped with a single antenna. Furthermore, Kronecker product-based beamforming codebooks are employed [49]. The total number of samples available in the dataset is 38038, from which n samples are reserved as labeled data, and the remaining $N = 38038 - n$ samples are considered as unlabeled data.

¹<https://www.remcom.com/wireless-insite-em-propagation-software>

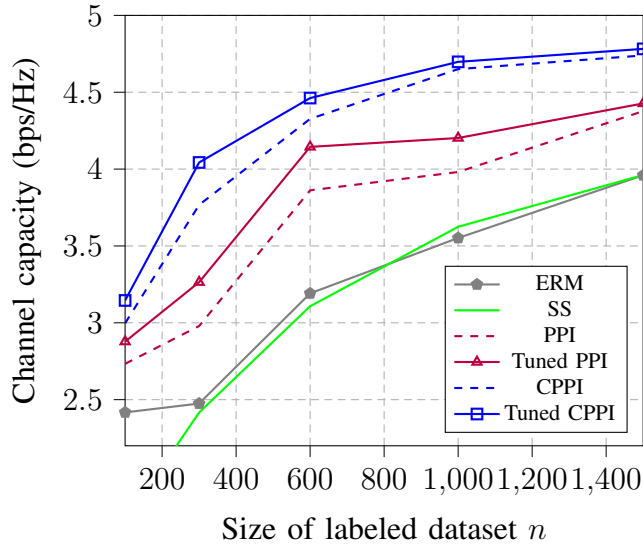


Fig. 7. Channel capacity as a function of the size of labeled dataset n when the number of BS antennas is fixed to $N^{TX} = 200$.

In Fig. 6, we report the performance in terms of the channel capacity $\log_2(1 + \text{SNR})$, where the SNR is evaluated as (29) for all schemes except for the perfect CSI case, which uses Y in (28). We vary the number of transmit antennas at the BS while setting the size of the labeled dataset to $n = 300$ and $n = 3000$. It is observed that the proposed tuned CPPI outperforms all the benchmark schemes while exhibiting the same performance as CPPI when the number of labeled data points, n , is large enough. We also remark from the figure that conventional semi-supervised (SS) learning, which does not take into consideration the bias from the trained prediction models, fails to provide any gains by incorporating the unlabeled data. Finally, we note that PPI and tuned PPI, while offering some gain as compared to ERM, do not reach the performance of tuned CPPI.

To further elaborate on the impact of the number of labeled data points, n , we report the channel capacity as a function of the labeled dataset size n in Fig. 7. As seen, the proposed tuned PPI provides the best performance among all the benchmark schemes, with more significant gains for smaller values of the labeled dataset size n . In fact, in this regime, the trained CKM is not sufficiently accurate, and tuned CPPI, which can adapt to the quality of the trained models via the tuning parameter λ , yields better performance.

VII. PREDICTION-POWERED RSSI LOCALIZATION

In this section, we consider the problem of indoor localization based on received signal strength information (RSSI) [50]. RSSI-based localization is a popular positioning technique [6], [30], in which RSS measurements from multiple access points (APs) are used to infer the location of a user equipment (UE). We investigate the scenario in which a labeled dataset containing RSSI measurements X and the corresponding UE locations Y is available, along with an unlabeled dataset with only RSSI measurements \tilde{X} . For instance, the unlabeled dataset could contain RSS measurements collected by volunteers who do not reveal their location information [10].

A. System Model

We consider an indoor environment m access points (APs) [36]. Given a dataset $\mathcal{D} = \{(X_i, Y_i)\}_{i=1}^n$ of RSSI measurements $X_i \in \mathbb{R}^m$ and the corresponding location information (longitude and latitude) $Y_i \in \mathbb{R}^2$, as well as an unlabeled dataset consisting of RSSI measurements $\tilde{X}_i \in \mathbb{R}^m$.

As in [51], the goal is to train an extreme learning machine (ELM) regression model to predict the label Y given RSSI measurements X [52], [53]. An ELM model is a single hidden layer neural network, in which the weights connecting the hidden layer and the output layer are optimized, while other parameters are randomly initialized and kept fixed. With p neurons in the hidden layer, define as $W \in \mathbb{R}^{p \times m}$ the weight matrix between the input and the hidden layer, and as $b \in \mathbb{R}^p$ the bias vector at the hidden layer. The ELM model predicts the label as [53]

$$\hat{Y} = [h(X)^T \theta_1, h(X)^T \theta_2]^T, \quad (35)$$

where $\sigma(\cdot)$ is an activation function; $\theta = [\theta_1^T, \theta_2^T]^T \in \mathbb{R}^{2p}$ is a parameter vector to be optimized; and $h(X) = \sigma(WX + b)$. The loss function is given as [53]

$$\ell_\theta(X, Y) = \sum_{j=1}^2 \mathbb{E} [(Y[j] - h(X)^T \theta_j)^2] + \gamma \sum_{j=1}^2 \|\theta_j\|_2^2, \quad (36)$$

with $Y[j]$ being the j -th entry of vector Y .

In order to reduce the data requirements for training the ELM model, we leverage the availability of unlabeled data \tilde{X} by using ML prediction models. Specifically, the PPI model $f(X)$ and the CPPI models $\{f^{(k)}(X)\}$ are implemented here as a fully connected neural network with three hidden layers of size 256, 128, and 32, respectively, with a LeakyRelu activation function.

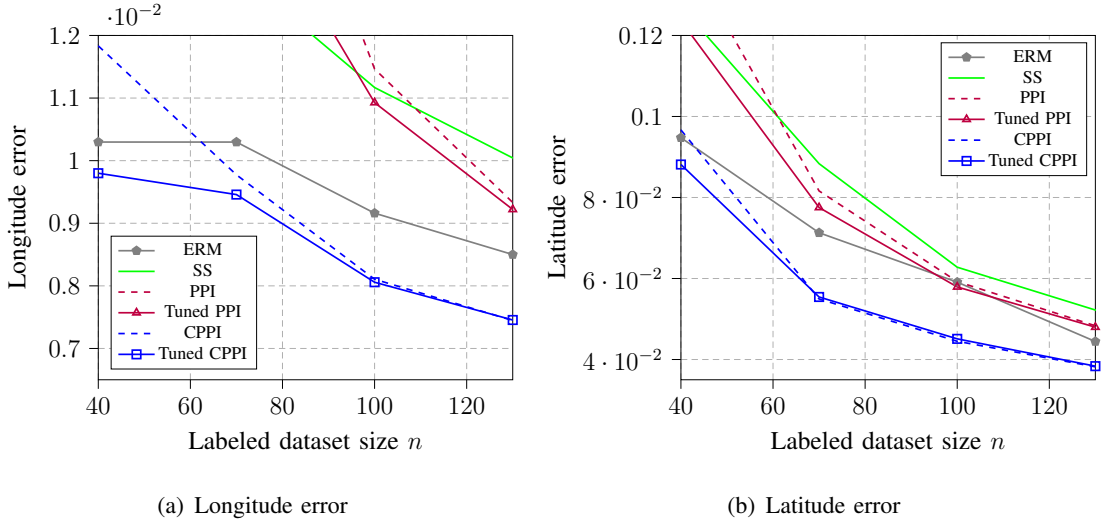


Fig. 8. Localization error as a function labeled dataset size n . the results are averaged over 100 trials.

B. Numerical Results

We compare the performance of tuned CPPI with the benchmark schemes using a real dataset from [54], which contains indoor RSS measurements from multiple WiFi APs with the corresponding longitude and latitude information in several floors and three buildings. The dataset can be used for both regression, predicting longitude and latitude, and classification, predicting floor number and building. Since our focus here is regression, we consider in our experiments a subset of the data corresponding to one floor in a specific building. The considered subset contains 2097 samples, from which 20% of samples are reserved for testing. Given a labeled data size n , the training data is randomly divided into a labeled dataset of size n and an unlabeled dataset of size N . For PPI and tuned PPI, the labeled dataset is divided into two equal parts for fitting model $f(X)$ and for computing the rectifier term.

Fig. 8 reports longitude and latitude errors of all schemes as a function of the labeled dataset size n . We note that the tuned CPPI scheme guarantees the best performance and outperforms CPPI for smaller values of n . Moreover, both CPPI and tuned CPPI provide a significant gain as compared to ERM, while PPI, tuned PPI, and conventional SS (with $\gamma = 1$) perform worse than ERM.

VIII. CONCLUSION

In this work, we have investigated the potential benefits of prediction-powered inference (PPI) for wireless systems. PPI leverages predictions generated by ML models to augment labeled data, while carefully considering their inherent prediction bias. PPI and its variant tuned PPI assume the existence of a pre-trained prediction model, while cross PPI (CPPI) alleviates this assumption by leveraging labeled data for the tasks of training prediction models and of correcting the inherent bias.

We have specifically explored two potential applications of the framework within wireless systems: CKM-based beam alignment and RSSI-based indoor localization. In addition, we have introduced a novel variant of PPI, tuned CPPI, which endows CPPI with the capacity to tailor based on the accuracy of the trained prediction models. We have compared the performance of all PPI variants with ERM, a baseline scheme reliant solely on labeled data, and with conventional semi-supervised learning, which overlooks the prediction bias. Numerical results show the superiority of the proposed tuned CPPI scheme over all benchmark schemes.

PI schemes can benefit any wireless application in which labeled data are costly to obtain, but unlabeled data are available. Identifying and investigating these applications represents a promising direction for future research. Of particular interest are applications that leverage digital twins of the physical system to augment the datasets [55]–[57]. At a methodological level, extensions of the proposed tuned CPPI to active learning methods [58] could be addressed by further research.

APPENDIX

BOOTSTRAP-BASED ESTIMATION

Here, we describe the bootstrap approach to estimate the covariance matrix $\text{Var}(\nabla \ell_{\theta^*}^{\bar{f}})$ and the cross-covariance matrix $\text{Cov}(\nabla \ell_{\theta^*}, \nabla \ell_{\theta^*}^{\bar{f}})$. The approach consists of simulating several runs of the training process and averaging their results. For each run $b \in \{1, \dots, B\}$, we sample $n - n/K$ data points from the labeled dataset, denoted by \mathcal{I}_b , and train a model $f^{(b)}(X)$ using these data points. The predictions from the trained models $\{f^{(b)}(X)\}_{b=1}^B$ are leveraged to estimate $\text{Var}(\nabla \ell_{\theta^*}^{\bar{f}})$ and $\text{Cov}(\nabla \ell_{\theta^*}, \nabla \ell_{\theta^*}^{\bar{f}})$.

The first covariance $\text{Var}(\nabla \ell_{\theta^*}^{\bar{f}})$ can be estimated using the unlabeled dataset as follows

$$\widehat{\text{Var}}(\nabla \ell_{\hat{\theta}}^{\bar{f}}) = \widehat{\text{Var}} \left(\nabla \ell_{\hat{\theta}}(\tilde{X}_i, \bar{f}(\tilde{X}_i)); i \in [N] \right), \quad (37)$$

where $\bar{f}(\tilde{X}_i) = \frac{1}{b} \sum_{b=1}^B f^{(b)}(\tilde{X}_i)$, and $\widehat{\text{Var}}(v_i; i \in \mathcal{I})$ denotes the empirical estimate of the covariance matrix of vectors v_i using data samples with indices $i \in \mathcal{I}$, i.e.,

$$\widehat{\text{Var}}(v_i; i \in \mathcal{I}) = \frac{1}{|\mathcal{I}|} \sum_{i \in \mathcal{I}} (v_i - \bar{v})(v_i - \bar{v})^T, \text{ with } \bar{v} = \frac{1}{|\mathcal{I}|} \sum_{i \in \mathcal{I}} v_i.$$

As for the cross-covariance $\text{Cov}(\nabla \ell_{\theta^*}, \nabla \ell_{\theta^*}^{\bar{f}})$, the labeled dataset is used as

$$\widehat{\text{Cov}}(\nabla \ell_{\hat{\theta}}, \nabla \ell_{\hat{\theta}}^{\bar{f}}) = \widehat{\text{Cov}} \left(\nabla \ell_{\hat{\theta}}(X_i, Y_i), \nabla \ell_{\hat{\theta}}(X_i, f^{(b)}(X_i)); i \in \{1, \dots, n\} \setminus I_b, b \in \{1, \dots, B\} \right), \quad (38)$$

where $\widehat{\text{Cov}}(u_i, v_i; i \in \mathcal{I})$ denotes the empirical estimate of the covariance matrix between vectors u_i and v_i using data samples with indices $i \in \mathcal{I}$, i.e.,

$$\widehat{\text{Cov}}(u_i, v_i; i \in \mathcal{I}) = \frac{1}{|\mathcal{I}|} \sum_{i \in \mathcal{I}} (u_i - \bar{u})(v_i - \bar{v})^T,$$

with $\bar{u} = \frac{1}{|\mathcal{I}|} \sum_{i \in \mathcal{I}} u_i$ and $\bar{v} = \frac{1}{|\mathcal{I}|} \sum_{i \in \mathcal{I}} v_i$. Note that the bootstrapped models are not averaged when estimating $\text{Cov}(\nabla \ell_{\theta^*}, \nabla \ell_{\theta^*}^{\bar{f}})$ in (38) to ensure that each sample from the labeled dataset used to compute $\nabla \ell_{\hat{\theta}}(X_i, Y_i)$ is independent of the samples $f^{(b)}$ was trained on.

REFERENCES

- [1] Y. Sun, M. Peng, Y. Zhou, Y. Huang, and S. Mao, “Application of machine learning in wireless networks: Key techniques and open issues,” *IEEE Communications Surveys & Tutorials*, vol. 21, no. 4, pp. 3072–3108, 2019.
- [2] O. Simeone, “A very brief introduction to machine learning with applications to communication systems,” *IEEE Transactions on Cognitive Communications and Networking*, vol. 4, no. 4, pp. 648–664, 2018.
- [3] Q. Mao, F. Hu, and Q. Hao, “Deep learning for intelligent wireless networks: A comprehensive survey,” *IEEE Communications Surveys & Tutorials*, vol. 20, no. 4, pp. 2595–2621, 2018.
- [4] J. Liao, J. Zhao, F. Gao, and G. Y. Li, “Deep learning aided low complex sphere decoding for MIMO detection,” *IEEE Transactions on Communications*, vol. 70, no. 12, pp. 8046–8059, 2022.
- [5] O. Shental and J. Hoydis, “Machine LLRning”: Learning to softly demodulate,” in *Proc. IEEE Globecom Workshops (GC Wkshps)*, 2019, pp. 1–7.
- [6] K. Wu, J. Xiao, Y. Yi, D. Chen, X. Luo, and L. M. Ni, “CSI-based indoor localization,” *IEEE Transactions on Parallel and Distributed Systems*, vol. 24, no. 7, pp. 1300–1309, 2013.
- [7] B. Zhang, H. Sifaou, and G. Y. Li, “CSI-fingerprinting indoor localization via attention-augmented residual convolutional neural network,” *IEEE Transactions on Wireless Communications*, vol. 22, no. 8, pp. 5583–5597, 2023.
- [8] X. Yang, Z. Song, I. King, and Z. Xu, “A survey on deep semi-supervised learning,” *IEEE Transactions on Knowledge and Data Engineering*, vol. 35, no. 9, pp. 8934–8954, 2022.
- [9] N. Van Huynh, J. Wang, H. Du, D. T. Hoang, D. Niyato, D. N. Nguyen, D. I. Kim, and K. B. Letaief, “Generative AI for physical layer communications: A survey,” *IEEE Transactions on Cognitive Communications and Networking*, 2024.
- [10] S. Li, Z. Tang, K. S. Kim, and J. S. Smith, “Exploiting unlabeled RSSI fingerprints in multi-building and multi-floor indoor localization through deep semi-supervised learning based on mean teacher,” in *Proc. International Symposium on Computing and Networking (CANDAR)*, 2023, pp. 155–160.

- [11] J. Yoo and K. H. Johansson, “Semi-supervised learning for mobile robot localization using wireless signal strengths,” in *Proc. International Conference on Indoor Positioning and Indoor Navigation (IPIN)*, 2017, pp. 1–8.
- [12] S. Kim, M. So, N. Lee, and S. Hong, “Semi-supervised learning detector for MU-MIMO systems with one-bit ADCs,” in *Proc. IEEE International Conference on Communications Workshops (ICC Workshops)*, 2019, pp. 1–6.
- [13] L. V. Nguyen, D. T. Ngo, N. H. Tran, A. L. Swindlehurst, and D. H. Nguyen, “Supervised and semi-supervised learning for MIMO blind detection with low-resolution ADCs,” *IEEE Transactions on Wireless Communications*, vol. 19, no. 4, pp. 2427–2442, 2020.
- [14] E. Nayebi and B. D. Rao, “Semi-blind channel estimation for multiuser massive MIMO systems,” *IEEE Transactions on Signal Processing*, vol. 66, no. 2, pp. 540–553, 2017.
- [15] J. A. Soares, K. S. Mayer, and D. S. Arantes, “Semi-supervised ML-based joint channel estimation and decoding for m-MIMO with Gaussian inference learning,” *IEEE Wireless Communications Letters*, vol. 12, no. 12, pp. 2123–2127, 2023.
- [16] M. Camelo, A. Shahid, J. Fontaine, F. A. P. De Figueiredo, E. De Poorter, I. Moerman, and S. Latre, “A semi-supervised learning approach towards automatic wireless technology recognition,” in *Proc. IEEE International Symposium on Dynamic Spectrum Access Networks (DySPAN)*, 2019, pp. 1–10.
- [17] J. Chen, S. Park, P. Popovski, H. V. Poor, and O. Simeone, “Neuromorphic split computing with wake-up radios: Architecture and design via digital twinning,” *arXiv preprint arXiv:2404.01815*, 2024.
- [18] A. N. Angelopoulos, S. Bates, C. Fannjiang, M. I. Jordan, and T. Zrnic, “Prediction-powered inference,” *Science*, vol. 382, no. 6671, pp. 669–674, 2023.
- [19] D.-H. Lee *et al.*, “Pseudo-label: The simple and efficient semi-supervised learning method for deep neural networks,” in *Proc. Workshop on Challenges in Representation Learning, ICML*, 2013, p. 896.
- [20] T. Raviv and N. Shlezinger, “Data augmentation for deep receivers,” *IEEE Transactions on Wireless Communications*, 2023.
- [21] A. N. Angelopoulos, J. C. Duchi, and T. Zrnic, “PPI++: Efficient prediction-powered inference,” *arXiv preprint arXiv:2311.01453*, 2023.
- [22] T. Zrnic and E. J. Candès, “Cross-prediction-powered inference,” *arXiv preprint arXiv:2309.16598*, 2023.
- [23] S. Qiao, W. Shen, Z. Zhang, B. Wang, and A. Yuille, “Deep co-training for semi-supervised image recognition,” in *Proc. European Conference on Computer Vision (ECCV)*, 2018, pp. 135–152.
- [24] M. Stone, “Cross-validation: A review,” *Statistics: A Journal of Theoretical and Applied Statistics*, vol. 9, no. 1, pp. 127–139, 1978.
- [25] ———, “Cross-validatory choice and assessment of statistical predictions,” *Journal of the royal statistical society: Series B (Methodological)*, vol. 36, no. 2, pp. 111–133, 1974.
- [26] K. M. Cohen, S. Park, O. Simeone, and S. Shamai, “Cross-validation conformal risk control,” *arXiv preprint arXiv:2401.11974*, 2024.
- [27] S. Park, K. M. Cohen, and O. Simeone, “Few-shot calibration of set predictors via meta-learned cross-validation-based conformal prediction,” *IEEE Transactions on Pattern Analysis and Machine Intelligence*, vol. 46, no. 1, pp. 280–291, 2024.
- [28] Y. Zeng and X. Xu, “Toward environment-aware 6G communications via channel knowledge map,” *IEEE Wireless Communications*, vol. 28, no. 3, pp. 84–91, 2021.
- [29] D. Wu, Y. Zeng, S. Jin, and R. Zhang, “Environment-aware and training-free beam alignment for mmwave massive MIMO via channel knowledge map,” in *Proc. IEEE International Conference on Communications Workshops (ICC Workshops)*, 2021, pp. 1–7.

- [30] A. S. Paul and E. A. Wan, "RSSI-based indoor localization and tracking using sigma-point Kalman smoothers," *IEEE Journal of Selected Topics in Signal Processing*, vol. 3, no. 5, pp. 860–873, 2009.
- [31] Y. Heng, Y. Zhang, A. Alkhateeb, and J. G. Andrews, "Site-specific beam alignment in 6G via deep learning," *arXiv preprint arXiv:2403.16186*, 2024.
- [32] W. Qian, F. Lauri, and F. Gechter, "Supervised and semi-supervised deep probabilistic models for indoor positioning problems," *Neurocomputing*, vol. 435, pp. 228–238, 2021.
- [33] R. Jiao, Y. Zhang, L. Ding, B. Xue, J. Zhang, R. Cai, and C. Jin, "Learning with limited annotations: a survey on deep semi-supervised learning for medical image segmentation," *Computers in Biology and Medicine*, vol. 169, p. 107840, 2024.
- [34] Y. Gao, B. Liu, Y. Zhu, L. Chen, M. Tan, X. Xiao, G. Yu, and Y. Guo, "Detection and recognition of ultrasound breast nodules based on semi-supervised deep learning: a powerful alternative strategy," *Quantitative Imaging in Medicine and Surgery*, vol. 11, no. 6, p. 2265, 2021.
- [35] O. Chapelle, B. Schölkopf, and A. Zien, *Semi-supervised learning*. The MIT Press, 2006.
- [36] M. Nabati, H. Navidan, R. Shahbazian, S. A. Ghorashi, and D. Windridge, "Using synthetic data to enhance the accuracy of fingerprint-based localization: A deep learning approach," *IEEE Sensors Letters*, vol. 4, no. 4, pp. 1–4, 2020.
- [37] A. W. Van der Vaart, *Asymptotic statistics*. Cambridge University Press, 1998.
- [38] T. K. Ho, "Random decision forests," in *Proc. of International Conference on Document Analysis and Recognition*, vol. 1. IEEE, 1995, pp. 278–282.
- [39] G. Barrie Wetherill, P. Duncombe, M. Kenward, J. Kölnerström, S. R. Paul, and B. J. Vowden, *Choosing a regression model*. Springer Netherlands, 1986, pp. 230–248.
- [40] M. Giordani, M. Polese, A. Roy, D. Castor, and M. Zorzi, "A tutorial on beam management for 3GPP NR at mmWave frequencies," *IEEE Communications Surveys & Tutorials*, vol. 21, no. 1, pp. 173–196, 2018.
- [41] J. Yang, W. Zhu, M. Tao, and S. Sun, "Hierarchical beam alignment for millimeter-wave communication systems: A deep learning approach," *IEEE Transactions on Wireless Communications*, vol. 23, no. 4, pp. 3541–3556, 2024.
- [42] W. Zhang, H. Li, P. Liu, S. Wei, W. Cheng, and W. Wang, "Adaptive beam alignment method for millimeter-wave massive MIMO communication systems," *Physical Communication*, vol. 41, p. 101101, 2020.
- [43] S. Kutty and D. Sen, "Beamforming for millimeter wave communications: An inclusive survey," *IEEE Communications Surveys & Tutorials*, vol. 18, no. 2, pp. 949–973, 2015.
- [44] C. Williams and M. Seeger, "Using the Nyström method to speed up kernel machines," in *Proc. Advances in Neural Information Processing Systems*, 2001, pp. 682–688.
- [45] S. Menard, *Applied logistic regression analysis*. Sage, 2002, no. 106.
- [46] M. Ribeiro, N. Nunes, V. Nisi, and J. Schöning, "Passive Wi-Fi monitoring in the wild: a long-term study across multiple location typologies," *Personal and Ubiquitous Computing*, vol. 26, no. 3, pp. 505–519, 2022.
- [47] A. E. Redondi and M. Cesana, "Building up knowledge through passive WiFi probes," *Computer Communications*, vol. 117, pp. 1–12, 2018.
- [48] B. Xu, N. Wang, T. Chen, and M. Li, "Empirical evaluation of rectified activations in convolutional network," *arXiv preprint arXiv:1505.00853*, 2015.
- [49] Y. Xie, S. Jin, J. Wang, Y. Zhu, X. Gao, and Y. Huang, "A limited feedback scheme for 3D multiuser MIMO based on Kronecker product codebook," in *Proc. IEEE International Symposium on Personal, Indoor, and Mobile Radio Communications (PIMRC)*, 2013, pp. 1130–1135.
- [50] S. Sadowski and P. Spachos, "RSSI-based indoor localization with the internet of things," *IEEE Access*, vol. 6, pp. 30149–30161, 2018.

- [51] J. Yan, G. Qi, B. Kang, X. Wu, and H. Liu, “Extreme learning machine for accurate indoor localization using RSSI fingerprints in multifloor environments,” *IEEE Internet of Things Journal*, vol. 8, no. 19, pp. 14 623–14 637, 2021.
- [52] G.-B. Huang, Q.-Y. Zhu, and C.-K. Siew, “Extreme learning machine: theory and applications,” *Neurocomputing*, vol. 70, no. 1-3, pp. 489–501, 2006.
- [53] G.-B. Huang, H. Zhou, X. Ding, and R. Zhang, “Extreme learning machine for regression and multiclass classification,” *IEEE Transactions on Systems, Man, and Cybernetics, Part B (Cybernetics)*, vol. 42, no. 2, pp. 513–529, 2011.
- [54] J. Torres-Sospedra, R. Montoliu, A. Martínez-Usó, J. P. Avariento, T. J. Arnau, M. Benedito-Bordonau, and J. Huerta, “UJIIndoorLoc: A new multi-building and multi-floor database for WLAN fingerprint-based indoor localization problems,” in *Proc. International Conference on Indoor Positioning and Indoor Navigation (IPIN)*, 2014, pp. 261–270.
- [55] S. Jiang and A. Alkhateeb, “Digital twin based beam prediction: Can we train in the digital world and deploy in reality?” in *Proc. IEEE International Conference on Communications Workshops (ICC Workshops)*, 2023, pp. 36–41.
- [56] C. Ruah, O. Simeone, J. Hoydis, and B. Al-Hashimi, “Calibrating wireless ray tracing for digital twinning using local phase error estimates,” *arXiv preprint arXiv:2312.12625*, 2023.
- [57] H. Luo and A. Alkhateeb, “Digital twin aided compressive sensing: Enabling site-specific mimo hybrid precoding,” *arXiv preprint arXiv:2405.07115*, 2024.
- [58] T. Zrnic and E. J. Candès, “Active statistical inference,” *arXiv preprint arXiv:2403.03208*, 2024.